Characterization of Heparin Binding of Human Extracellular Superoxide Dismutase[†]

Aivar Lookene,[‡] Peter Stenlund,[§] and Lena A. E. Tibell*[,§]

Department of Biochemistry and Department of Medical Biochemistry and Biophysics, Umeå University, S-901 87 Umeå, Sweden, and Institute of Chemical Physics and Biophysics, Tallinn, Estonia

Received June 30, 1999; Revised Manuscript Received September 29, 1999

ABSTRACT: The C-terminal domain of human extracellular superoxide dismutase (hEC-SOD) plays a crucial role in the protein's interaction with heparin. Here we investigated this interaction in more detail by comparing the heparin-binding characteristics of two variants of hEC-SOD: the two fusion proteins containing the hEC-SOD C-terminal domain and a synthetic peptide homologous to the C-terminal. The interaction studies were performed using a surface plasmon resonance based technique on a BIAcore system. It should be emphasized that this is a model system. However, the kinetic constants, as measured, are valid in a comparative sense. Comparison of affinities for size-fractionated heparins revealed that octa- or decasaccharides are the smallest heparin fragments that can efficiently interact with the C-terminal domain of hEC-SOD. At physiological salt concentration, and pH 7.4, the hEC-SOD/heparin interaction was found to be of a high-affinity type, with an equilibrium dissociation constant, K_d, of 0.12 μM, which is 700 and 10−20 times lower than the K_d values for the synthetic peptide and the fusion proteins, respectively. However, when an α-helical structure was induced in the synthetic peptide, by addition of 10% trifluoroethanol, the K_d decreased to 0.64 μM. The differences in the K_d values were mainly governed by differences in the association rate constants (k_{ass}). The hEC-SOD/heparin interaction itself was found to have a fairly high dissociation rate constant (0.1 s^{-1}), and a very high association rate constant (8×10^5 M^{-1} s^{-1}), suggesting that the interaction is mainly controlled by the association. These results together with circular dichroism spectra of the synthetic peptide suggest that an α-helical structure in the C-terminal is essential for optimal binding to heparin and that other parts of hEC-SOD moderate the affinity. Our data also demonstrate that the tetramerization itself does not substantially increase the affinity.

Oligosaccharides and glycosaminoglycans (GAG's)[1] are decorating the cell surface of most mammalian cells, where they are involved in a range of fundamental cellular activities (*1*). Critical for most of these activities are protein−oligosaccharide interactions, which often are of a specific nature. Among the protein−GAG interactions that have been studied, heparin and heparan sulfate binding protein complexes are best characterized, mainly because of the commercial availability of heparin. However, the biological ligand in most cases is heparan sulfate. A wide range of extracellular proteins has been shown to bind to both heparin and heparan sulfate, and the functions of heparan sulfate are correspondingly diverse. Functions already described at a molecular level include protein activation, localization and protection of bound proteins, chaperone activity during secretion, and co-receptor roles (*1*).

The consequences of the interaction of many proteins with heparin have been characterized, but the mechanisms by which heparin operates at the molecular (structural) level remain unclear. Considerable effort has been invested in characterizing the nature of the protein−heparin interaction. However, these studies have been hampered by the heterogeneity of heparin and heparan sulfate, and the X-ray structure of a protein−heparin complex has been determined only in one case, the fibroblast growth factor (*2*, *3*).

Superoxide dismutase (SOD) enzymes are metalloenzymes, present in most aerobic organisms, which catalyze the dismutation of superoxide radicals. Mammalian cells produce two different types of copper- and zinc-containing SODs: one intracellular form (CuZn-SOD) and one extracellular form (EC-SOD). One of the characteristic properties of EC-SOD is that it binds to sulfated glycosaminoglycans, and the affinity of human EC-SOD (hEC-SOD) for heparin and heparan sulfate is well documented (*4*−*6*). The C-terminal domain was proposed at an early stage to be responsible for this interaction (*7*), and this hypothesis has been confirmed by a wide range of experiments (*6*, *8*−*14*).

To investigate structural aspects of the interaction between the C-terminal domain of hEC-SOD and heparin, we recently constructed and studied a fusion protein comprising the 27

[†] This work was supported by grants from Carl Tryggers Stiftelse, Stiftelsen Lars Hiertas minne, Magnus Bergvalls Stiftelse, Ollie och Elof Ericssons Stiftelse, JC Kempes Minnes Stipendiefond, and Estonian Science Foundation.

* Correspondence should be addressed to this author at the Department of Biochemistry, Umeå University, S-901 87 Umeå, Sweden. Telephone: 46-90-786 76 33. Fax: 46-90-786 76 61. E-mail: lena.tibell@chem.umu.se.

[‡] Institute of Chemical Physics and Biophysics, Tallinn, and Department of Medical Biochemistry and Biophysics, Umeå University.

[§] Department of Biochemistry, Umeå University.

[1] Abbreviations: CuZn-SOD, Cu- and Zn-containing superoxide dismutase (EC 1.15.1.1); EC-SOD, extracellular Cu- and Zn-containing superoxide dismutase (EC 1.15.1.1); FusCC, C-terminal fusion of the 25 C-terminal amino acids from human EC-SOD to the C-terminal of HCAII; GAG, glycosaminoglycan; HCAII, human carbonic anhydrase II (EC 4.2.1.1); ngEC-SOD, nonglycosylated recombinant human EC-SOD; rhEC-SOD, recombinant human EC-SOD; pseudoEC-SOD, 49 N-terminal and 25 C-terminal amino acids of human EC-SOD fused to the N- and C-terminals of human CuZn-SOD, respectively; SOD, superoxide dismutase; TFE, 2,2,2-trifluoroethanol.

10.1021/bi991512x CCC: $19.00
Published on Web 12/14/1999

C-terminal amino acids of hEC-SOD linked to the C-terminal of the totally unrelated monomeric protein, human carbonic anhydrase II (HCAII). The resulting construct, FusCC, was shown to be a monomeric protein, which bound to heparin−Sepharose with approximately the same affinity as the tetrameric hEC-SOD. Further, NMR data showed that the C-terminals of both hEC-SOD and FusCC move independently from the rest of the protein. The NMR data also indicated that the central part of the C-terminal domain is involved in a dynamic equilibrium exchange between different conformations, that the C-terminal domain in FusCC and hEC-SOD binds to heparin, and that arginine side chains take part in the binding (*6*). The C-terminal domain is apparently essential and sufficient for binding to heparin−sulfate. However, nothing is known about how the binding is influenced by interactions of the C-terminal domain with other parts of the protein.

In the study presented here, we have measured key kinetic parameters for interactions between heparin and various proteins containing the C-terminal domain, and a synthesized peptide corresponding to the C-terminal domain. The proteins used in this study were the following: recombinant human EC-SOD (rhEC-SOD), a nonglycosylated variant of rhEC-SOD (ngEC-SOD), pseudoEC-SOD (a fusion protein comprising the N- and C-terminal domains of hEC-SOD fused to the N- and C-terminals of hCuZn-SOD), and FusCC. Comparison of these factors has allowed us to analyze the dynamics of the complex formed between heparin and the C-terminal domain, and to make inferences concerning the involvement of other parts of the protein in stabilizing the interaction.

MATERIALS AND METHODS

Chemicals and Proteins. The isolated heparin fragments used in the BIAcore and CD studies were a kind gift from Per Østergaard, Novo Nordisk, Denmark; the decasaccharide was purified by affinity chromatography on LPL-Sepharose according to ref *15*. An amino-coupling kit and CM5 sensor chips were obtained from BIAcore, Uppsala, Sweden. Streptavidin, avidin, and 2,2,2-trifluoroethanol were from Sigma. A synthetic peptide with a sequence homologous to the C-terminal domain of hEC-SOD, but with the substitution of Cys219 by Ser (to avoid disulfide bridge formation), N-GLWERQASEHSERKKRRRESESKAA-C, was synthesized by Alta Bioscience, The University of Birmingham, U.K.

Recombinant human rhEC-SOD and a nonglycosylated variant of the same enzyme, ngEC-SOD (*16*), were generous gifts from Symbicom AB. The construction and purification of the fusion proteins, FusCC and pseudoEC-SOD, have been described earlier (*6, 14*).

Analytical Heparin−Sepharose Chromatography. The chromatography was carried out in a 2.5 mL heparin−Sepharose column using an equilibrium buffer composed of 15 mM sodium cacodylate, pH 6.5, containing 50 mM NaCl. Bound proteins/peptide was eluted using a gradient (solid line) of 50 mM to 1 M NaCl in the equilibration buffer.

Circular Dichroism (CD). Far-UV CD spectra of the synthetic peptide were recorded at 25 °C on a CD6 spectrodichrograph (Jobin-Yvon Instruments SA, Longjumeau, France) in a 0.5 mm path-length cell with a peptide concentration of 72 μM. For the titration experiments, the synthetic peptide was dissolved in 0−40% v/v TFE and 5 mM sodium phosphate, pH 7.6. The titrations with the decasaccharide and 20-mer heparin fragment were performed in 5 mM sodium phophate, pH 7.6, and the saccharide concentration ranged from 0 to 10 times the molar concentration of the synthetic peptide. Concentration independence of the CD signal was also established for the synthetic peptide.

Determination of Kinetic Constants. Experiments were performed on a BIAcore2000 instrument. Streptavidin or avidin were coupled through amino groups to the activated carboxyl groups on the dextran matrix of CM5 sensor chips according to the general procedures recommended by the manufacturer of the instrument. The biosensor measures refractive index changes close to the dextran layer and are proportional to the amount of bound molecules. After the immobilization, the change in response, expressed in arbitrary units, RU (response units), ranged between 3000 and 5000. Biotinylated heparin was then bound to the covalently immobilized avidin or streptavidin, and the proteins were injected over the layer at a constant flow rate.

The protein/heparin interactions were performed in 10 mM Hepes, 0.15 M NaCl, pH 7.4 at 25° C, and the protein concentrations varied between 1 nM and 200 μM. The effect of ionic strength on the protein/heparin interaction was studied by varying the concentration of NaCl in the binding buffer. After each binding experiment, the surface of the sensor chip was regenerated by washing with 1 M NaCl or 0.1% SDS.

To determine association and dissociation rate constants, k_{ass} and k_{diss}, respectively, the sensorgrams were analyzed using BIA evaluation software. The equilibrium constant, K_d, was determined from the equation:

$$\Delta R_{eq} = \frac{\Delta R_{max} C}{K_d + C} + bC$$

where ΔR_{eq} is the increase of the response values at equilibrium, ΔR_{max} is the capacity of the immobilized heparin to bind a protein (the number of binding sites), C is the concentration of the injected protein, and b is a proportionality constant representing nonspecific binding (*17*)

Competition studies with heparin fragments were performed according to methods described in a previous study (*17*). The data were analyzed by nonlinear regression using the FIG.P version 2.5 program (Biosoft, Cambridge, U.K.).

RESULTS

The heparin binding properties of the proteins were measured and compared on heparin−Sepharose (Figure 1). The rhEC-SOD (tetramer) and FusCC (monomer) eluted at approximately the same NaCl concentration (0.55 M) as the native hEC-SOD type C (tetramer) (*16*). The ngEC-SOD (tetramer) bound more strongly and eluted at 0.62 M NaCl whereas pseudoEC-SOD (tetramer) and the synthetic peptide bound more weakly, eluting at 0.45 and 0.38 M NaCl, respectively (Figure 1).

The BIAcore biosensor system was used to measure the kinetic constants. All studied proteins were able to bind only to highly sulfated heparin. However, HCAII and CuZn-SOD,

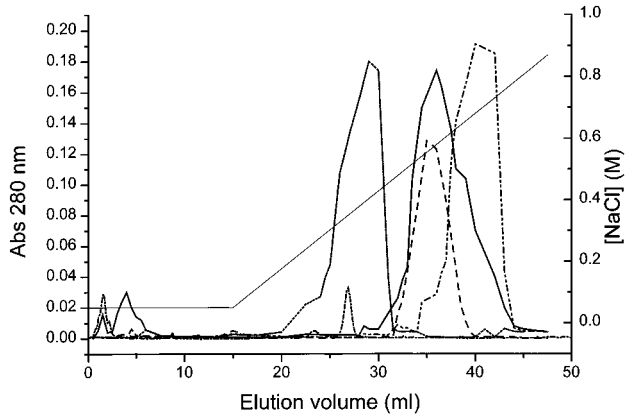

FIGURE 1: Heparin−Sepharose chromatography of rhEC-SOD (solid line), ngEC-SOD (− ·· −), pseudoEC-SOD (···), FusCC (- - -), and the synthetic peptide (− · −).

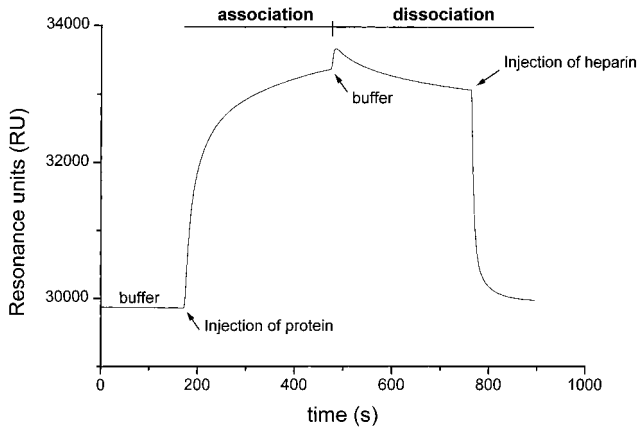

FIGURE 2: Sensorgram demonstrating the dramatic increase in the dissociation rate of rhEC-SOD from immobilized heparin following injection of free heparin. 200 nM rhEC-SOD was initially equilibrated with the sensorchip layer with immobilized heparin. In the dissociation phase, first only buffer was passed; then 10 IU/mL heparin was injected. The arrows show starting points of different injections. The association phase and dissociation phases are indicated.

which were used as fusion partners with the C-terminal domain of hEC-SOD, did not bind to heparin. For determination of the kinetic constants, we varied both the amount of immobilized heparin on the sensor chips and the concentrations of the injected proteins. We found several general properties in the binding kinetics which were similar among all the studied proteins. First, at low protein concentrations (<0.5 μM), the association followed simple bimolecular kinetics. At higher protein concentrations, the kinetics were better described by a two binding site model. Second, at surface densities ranging from 0.05 to 2 ng/mm^2, the association kinetics were not significantly dependent on the amount of immobilized heparin. Third, addition of free heparin during the dissociation phase markedly increased the dissociation rate, suggesting that avid rebinding of the dissociated proteins occurs (Figure 2). The association rate constants were determined at low concentrations (<500 nM), where the interactions were sufficiently well described by a single binding site model.

The equilibrium dissociation constants (K_d) were calculated from the relationships between steady-state response values (ΔR_{eq}) and protein concentrations. The number of binding sites on the immobilized heparin chains, expressed as the ratio $\Delta R_{max}/M_w$, where R_{max} represents the degree of saturation and M_w is molecular weight, were almost equal for rhEC-SOD, ngEC-SOD, FusCC, and pseudoEC-SOD, while it was 7−8 times higher for the synthetic peptide. Thus, there were more binding sites available to the peptide than for the proteins.

Table 1: Kinetic Constants Characterizing the Binding of the Studied Proteins and Peptides to Immobilized Heparin

protein	K_d (μM)	k_{ass} (M^{-1} s^{-1})	k_{diss} (s^{-1})
hEC-SOD	0.12	8.0×10^5	0.10
ngEC-SOD	0.05	2.1×10^6	0.11
pseudoEC-SOD	1.00	4.8×10^4	0.05
FusCC	2.30	6.5×10^4	0.15
synthetic peptide	71	6.0×10^3	0.43
synthetic peptide in 10% v/v TFE	0.64	−	−

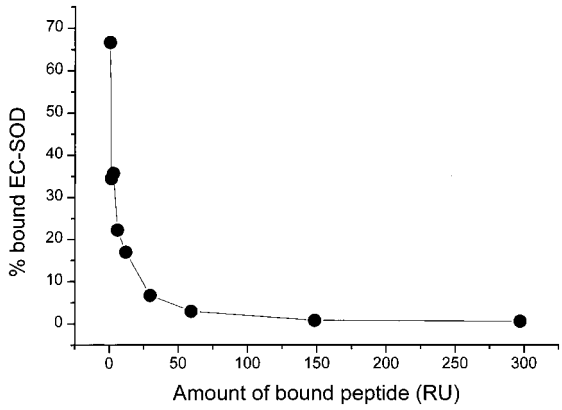

FIGURE 3: Competition between rhEC-SOD and the synthetic peptide homologous to the C-terminal end of hEC-SOD for binding heparin. Relative values for rhEC-SOD associated with heparin in the presence of different amounts of peptide are calculated as percentages of the binding of rhEC-SOD to heparin in the absence of the peptide.

The kinetic data for rhEC-SOD, ngEC-SOD, pseudoEC-SOD, FusCC, and the synthetic peptide are presented in Table 1. The data demonstrate that ngEC-SOD has the highest heparin affinity (K_d = 0.052 μM), largely because it has the highest association rate constant, k_{ass}. The absolute k_{ass} value (2×10^6 M^{-1} s^{-1}) for ngEC-SOD is very high and close to, but clearly below, the limit which can be properly characterized by the BIAcore system (10^7 M^{-1} s^{-1}) (*18*). Native glycosylated rhEC-SOD had somewhat lower affinity than ngEC-SOD. Nevertheless, the value for its K_d (0.12 μM) is still quite low and indicates a strong interaction. FusCC and pseudoEC-SOD had, respectively, 10 and 20 times higher K_d constants than rhEC-SOD. The synthetic peptide had the lowest affinity, due to a slow association rate ($k_{ass} = 6 \times 10^3$ M^{-1} s^{-1}). However, the affinity of the peptide increased markedly in the presence of 10% TFE. When the synthetic peptide was bound to the heparin sensorchips, it almost completely blocked the binding of 200 nM rhEC-SOD (Figure 3). Thus, the heparin-binding specificity of the peptide is not different from rhEC-SOD.

The dissociation rate was apparently slow (dissociation rate constant around 10^{-3}−10^{-4} s^{-1}) for all of the studied interactions, except those with the synthetic peptide. Injection of free heparin during the dissociation phase increased the k_{diss} values to approximately 0.1 s^{-1}, which is too fast for direct determination on the BIAcore system (Figure 2). Because of this, the dissociation rate constants were calcu-

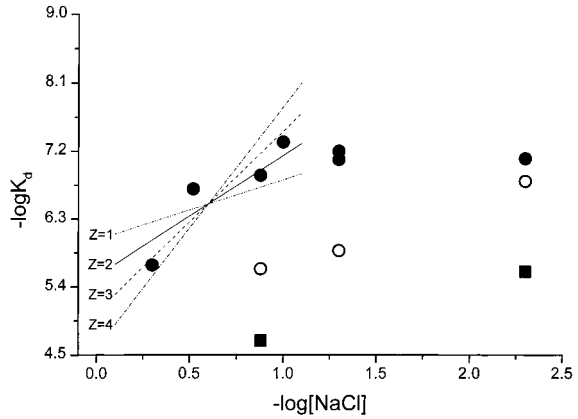

FIGURE 4: Effect of NaCl concentration on the interactions of heparin with EC-SOD and EC-SOD analogues. Effect of NaCl concentration on the equilibrium dissociation constant (K_d) of heparin interactions with rhEC-SOD (●), FusCC (○), and the synthetic peptide homologous to the C-terminal end of hEC-SOD (■). The indicated lines in the figure represents plots assuming that the number of displaced ions (z), in the equation $\log K_d = \log K_d^0 + z\Psi \log M^+$, must take an integer value (1, 2, 3, and 4) [z = the number of displaced ions, Ψ = the axial charge density on the polyelectrolyte ($\Psi = 0.8$ for heparin has been used), and K_d^0 = the contribution of nonionic interaction at $M^+ = 0$]. No correlation to the experimental data has been done.

lated from the equation: $k_{diss} = k_{ass}K_d$. The k_{diss} values for the various proteins did not differ much, suggesting that the interactions are mainly governed by the association stage.

The electrostatic nature of the heparin interaction was also investigated by varying the NaCl concentration in the binding studies. The K_d values for rhEC-SOD, FusCC, and the synthetic peptide were determined at a range of salt concentrations and were shown to be sensitive to salt, suggesting that it is largely electrostatic in nature (Figure 4).

The secondary structure prediction by GOR IV (*19*) for the C-terminal domain in rhEC-SOD indicates that it has a high degree of α-helix (68% α-helix, 24% coil and 8% other structures). This method has been shown to predict secondary structure in proteins well (*19*). Secondary predictions for small peptides are better performed by the Agadir method (*20*−*23*). This method predicts 16% helix for the synthetic peptide in water solution. This value can be compared to the helix content determined from a far-UV CD spectrum according to ref *24*. This theory assumes that any peptide which possesses 100% α-helix will have an ellipticity at 222 nm ($[\theta]_{222\ nm}$) equal to $-40\,000(1 - 2.5/n)$, where n is the number of amino acids in the peptide, including possible amide bonds at each blocked terminus. In the case of our synthetic peptide, the $[\theta]_{222\ nm}$ equals 5900 deg·cm^2·dmol, which would correspond to 16.5% α-helix, and remarkably similar to the predicted value (16%). Titration with decasaccharide or a 20-mer heparin fragment did not induce any significant change in the secondary structure (results not shown) in water. On the other hand TFE, which is a well-known helix-inducer (*25*), induces a typical α-helical conformation (Figure 5). Upon titration with TFE, we observed two common features: a sigmoidal increase in signal at 222 nm up to 40% TFE (Figure 5, inset graph), which corresponds to an α-helical content of 67%; and an isodichroic point near 203 nm (Figure 5). These results support that the helix induction is cooperative and that the helix−coil interchange is a two-state process (*26*). The BIAcore measurements were performed at 10% (v/v) TFE due to instrumental limitations. However, already at that TFE concentration the conformational change, 28% α-helix, was accompanied by a significant increase in binding affinity (K_d = 0.64) to the immobilized heparin, to a level close to that of rhEC-SOD (Table 1).

The dependency of the heparin interaction of rhEC-SOD and FusCC on the size of the heparin saccharide chain length was analyzed by evaluating the competition between size-

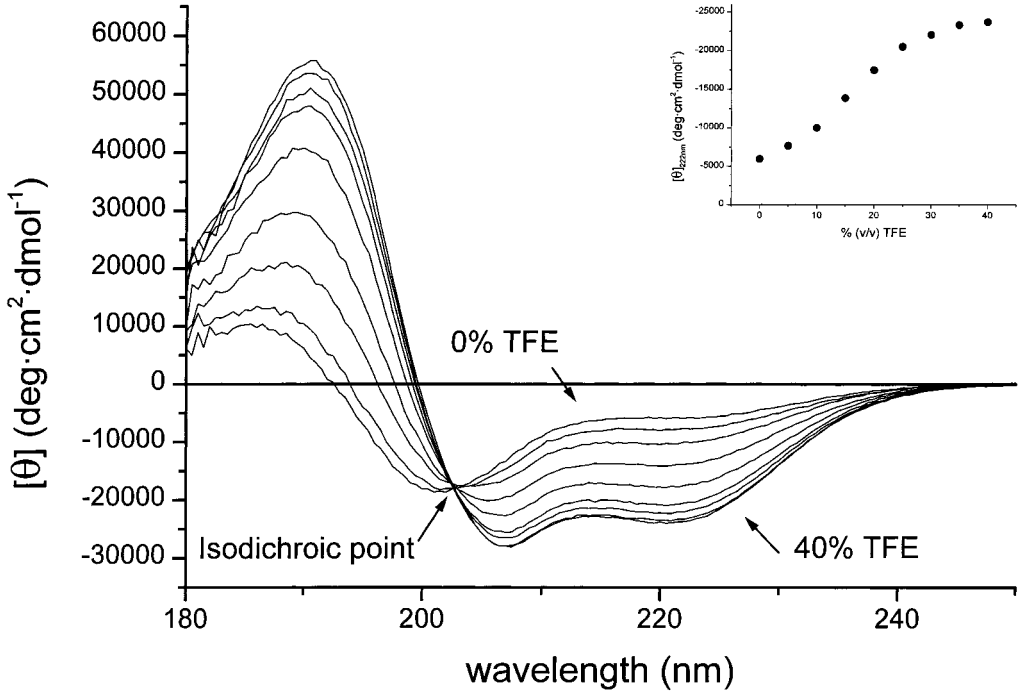

FIGURE 5: Circular dichroism spectra of the synthetic peptide (72 μM) in the far-ultraviolet region, in TFE concentrations ranging from 0 to 40% v/v. The inset graph shows that the change in CD signal (molar ellipticity) at 222 nm is sigmoidal upon titration with TFE (0−40% v/v).

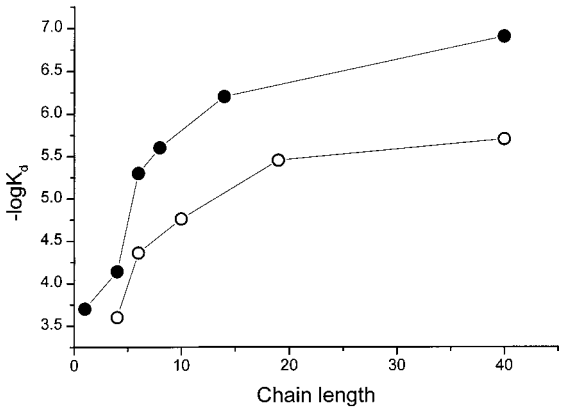

FIGURE 6: Effects of heparin chain length on protein−heparin equilibrium dissociation constants (K_d) for rhEC-SOD and FusCC. The dissociation constants were determined from competition studies between immobilized heparin and nonimmobilized size-fractionated oligosaccharides for the binding of rhEC-SOD (●) and FusCC (○). The chain length is expressed as number of monosaccharide units.

fractionated heparins and the immobilized heparin. The heparin fragments were preincubated with rhEC-SOD, and the mixture was injected over the sensorchip with the immobilized heparin. The relative decrease in protein binding was used to calculate corrsponding rate constants. The affinity plots, expressed as $-\log K_d$ versus heparin chain length, are shown in Figure 6. The shapes of the curves for rhEC-SOD and FusCC were very similar, although the absolute affinity values were higher for the native enzyme. The $-\log K_d$ was found to increase up to hexa- to decasaccharides, while for longer saccharides the effect of chain length was not so dramatic (Figure 6).

DISCUSSION

EC-SOD is among a growing number of proteins which have functions known to be moderated by heparin binding. In many cases, the consequences have been characterized, but the structure of the heparin−protein complex has been determined only in the case of basic fibroblast growth factor (*2*, *3*). In the absence of solid structural information regarding heparin−protein complexes, the mechanism by which heparin operates at the molecular level is still obscure. Several attempts to define consensus sequences for heparin binding at the protein level have been described, but none have been entirely successful. Cardin and Weintraub (*27*) identified sites of a fairly nonspecific character for heparin interaction, containing clusters of basic amino acids, and they also proposed that the polyanionic heparin might stabilize the conformation of the peptide upon binding. Investigation of known and predicted structures of heparin-interacting protein sequences led Margalit and co-workers to propose a structural, rather then a sequential, arrangement of two basic amino acid residues located 20 Å apart to be critical for heparin interaction (*28*). In a study by Mulloy and co-workers, heparin was shown to induce α-helix conformation in poly-L- (or D-) lysine synthetic polypeptides upon interaction (*29*). They could also identify the contact points in both heparin and the peptide, and the contact centers were found to be 17 Å apart.

The interaction of the C-terminal domains in hEC-SOD and heparin can be fitted in all these models. The C-terminal domain of hEC-SOD is strongly hydrophilic and rich in basic amino acids. There are eight basic amino acids found in a region predicted to form an α-helix, and R202 and R215 would have the same spatial arrangement as in the structural arrangement proposed by ref *28*. Further, the predicted α-helix is implied by previous NMR structural studies (*6*).

Heparin Requirements for Binding. An increase in affinity by increasing the heparin chain length can be caused either by gradual occupation of larger parts in the protein's heparin-binding region or, apparently, just by increasing the number of binding sites for the protein on the heparin chain. The latter phenomenon is known as the lattice effect and leads to a linear dependence for the graph K_d versus chain length (*30*). Since the dependencies on the heparin chain length for rhEC-SOD and FusCC were not linear, we speculate about the contribution of both effects. We propose that the relatively large change in the affinities observed from disaccharide to decasaccharide is mainly due to gradual occupancy of the heparin-binding regions of rhEC-SOD and FusCC. A much less pronounced increase of the affinity from decasaccharide to standard heparin may be caused by an increase in the number of binding sites on the heparin chain (Figure 6). Since the plots of heparin chain length/affinity were similar for EC-SOD and FussCC, we think that the sizes of the heparin-binding regions are comparable. In conclusion, tetramerization does not play a crucial role in the interaction.

Affinity Constants and Their Relation to Structure. The interactions between various heparin-binding proteins and heparin have previously been characterized and shown to range from low ($K_d = 10^{-4}-10^{-5}$ M), through medium ($K_d = 10^{-5}-10^{-7}$ M), to high affinity ($K_d = 10^{-7}-10^{-9}$ M) (*1*). The derived K_d of 0.12 μM for the heparin interaction of rhEC-SOD (Table 1) shows that it has high affinity. A very high value for the association rate constant and a slower dissociation rate constant characterize the interaction between rhEC-SOD and heparin. The combination of very fast association with slower (but still rapid) dissociation seems to be a general characteristic of protein−heparin interactions (*17*, *31*, *32*). The difference in heparin affinities (K_d) for the investigated proteins and the synthetic peptide therefore mainly appears to reflect a difference in k_{ass} values.

A slightly higher affinity for heparin, $K_d = 0.052$ μM, for the variant of hEC-SOD lacking the N-glycosylation site, ngEC-SOD (Figure 1), was observed. The slightly lower affinity of the glycosylated enzyme may be due to a repellent effect between the negatively charged carbohydrate moiety (at asparagine 89) on the protein and the negatively charged heparin. This also shows that other parts of the protein, in addition to the C-terminal domain, can affect the heparin interaction.

The kinetic constants for the heparin binding of the tetrameric fusion protein pseudoEC-SOD, $K_d = 1.0$ μM, and the monomeric fusion protein FusCC, $K_d = 2.3$ μM, suggest in both cases a weaker interaction than for rhEC-SOD (Table 1). The dissociation constants of the tetrameric pseudoEC-SOD and the monomeric FusCC differ by a factor of 2. However, the equilibrium dissociation constants for the tetrameric rhEC-SOD and pseudoEC-SOD differ by a factor of 10, and those of the tetrameric rhEC-SOD and the monomeric FusCC differ by a factor of 20. Thus, the differences in affinity cannot be simply an effect of the

number of subunits. Furthermore, the fact that the fusion proteins, FusCC and pseudoEC-SOD, show a similar binding constant, while rhEC-SOD binds10−20 times more strongly implies that the fusion partners (HCAII and CuZnSOD, respectively) do not contribute in the same way as the central domain of hEC-SOD to the heparin interaction.

We observed a discrepancy between the α-helical structure predicted with GOR IV (*19*) for the C-terminal domain of hEC-SOD, and the structure indicated by the CD spectrum in far-UV of the synthetic peptide. However, it is not uncommon that the structure of synthetic peptides is unordered when their sequences are derived from proteins (*33*). The Agadir method is better for secondary predictions of small peptides in water solution (*20*−*23*). The CD results are also in better agreement with prediction using this method (16% helix). This lack of defined structure could explain the fairly low affinity of the synthetic peptide for heparin (K_d = 71 μM) as compared to rhEC-SOD (K_d = 0.12 μM).

Mulloy and Ferran (*29*, *34*) have shown that heparin can induce α-helix in heparin binding synthetic peptides. However, in our case titration with a decasaccharide or a 20-mer heparin fragment did not induce any significant change in the secondary structure of the synthetic peptide in water (results not shown).

In an attempt to mimic the predicted α-helical structure of the C-terminal domain in rhEC-SOD, we introduced 10% (v/v) TFE in a series of binding experiments with the synthetic peptide. TFE/H_2O mixtures have been widely used to stabilize helices in synthetic peptides (*25*). The addition of TFE increased the affinity of the peptide for heparin approximately 100 times to a K_d of 0.64 μM (Table 1), which is close to the K_d of rhEC-SOD (0.12 μM). Interestingly, the far-UV CD spectra of the synthetic peptide show that addition of TFE to 10% (v/v) altered the conformation of the peptide from 16.5% to 28% α-helix (Figure 5). An obvious interpretation of these results is that stabilization of an α-helical conformation promotes heparin affinity. Because the synthetic peptides in 10% TFE and rhEC-SOD have similar affinities for heparin, we propose that the structure of the α-helix-containing peptide is similar to the native structure of the C-terminal domain in rhEC-SOD.

One can argue that the increased affinity might emanate from the fact that TFE is a less polar solvent then water and therefore strengthens electrostatic interactions. However, according to Luo and Baldwin (*25*), 10% TFE raised the pK_a for a model substance (*p*-hydroxybenzoic acid) by approximately 0.2. If we assume that this is a good model for the interaction between the negatively charged groups on heparin interacting with the positively charged groups on the C-terminal domain, 10% TFE would increase the binding affinity by a factor of 1.6 for each ion pair interaction. Therefore, the solvent effect by TFE can hardly explain the observed 100-fold increase in binding. In addition, we could not observe any effect on the CD spectra of heparin upon addition of TFE in the range 0−40%. This indicates that the effect of heparin on the affinity does not originate from an altered structure of the heparin molecule.

The results can be understood in a model having one high-affinity state where the peptide adopts a mainly α-helical conformation ($C_{high\ affinity}$) and one low-affinity state where the peptide is more unstructured ($C_{low\ affinity}$). In summary, the binding is described in Scheme 1.

Scheme 1

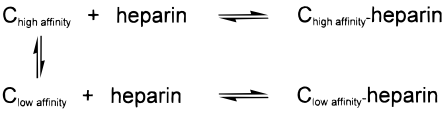

Results from titration of the synthetic peptide with TFE indicate that α-helix induction is not complete in 10% TFE (Figure 5, inset), and this might explain why the K_d of this peptide in TFE is approximately 5 times higher than that of hEC-SOD. Remarkably, the CD result at 40% TFE indicated 67% helix in the synthetic peptide, which is almost identical to the predicted α-helical content (68%) of the C-terminal domain in the intact rhEC-SOD. Oligomerization does not appear to contribute significantly to heparin affinity (Table 1). Therefore, we propose that the α-helical conformation of the C-terminal domain is the most important factor determining heparin affinity and that this conformation is stabilized by interactions with other parts of the rhEC-SOD molecule. The fusion partners in pseudoEC-SOD and FusCC seem to, at least partly, fulfill this stabilizing role.

Affinity As Measured by Heparin−*Sepharose Chromatography. Lessons from a Comparison with Steady-State Measurements*. When comparing these results with the results from heparin affinity chromatography of the corresponding proteins (showing that rhEC-SOD, FusCC, pseudoEC-SOD, and the synthetic peptide elute at concentrations of 0.55, 0.55, 0.45, and 0.38 M NaCl, respectively), the conclusion must be that heparin affinity is influenced by several factors. Our data illustrate that the salt concentration needed to elute proteins from heparin−Sepharose cannot always be used to estimate their relative heparin affinities. Although the BIAcore results show that rhEC-SOD has a clearly higher affinity than FusCC, pseudoEC-SOD, and the synthetic peptide at physiological salt concentration, all three proteins eluted from the heparin−Sepharose column at approximately the same sodium chloride concentration. Similar deviation between heparin chromatography data and direct affinity measurements has also been observed in previous studies (*35*, *36*). A possible explanation for this behavior is that the salt sensitivities of the proteins may differ; i.e., proteins that have the same affinity at one salt concentration may differ in affinity at other salt concentrations. Another explanation for the small differences in NaCl concentration required for elution of all proteins from heparin−Sepharose columns is, that under these conditions the dissociation rate constants are limiting. And since differences in K_{diss} values are small, the elution behavior is similar for all the different proteins.

Salt Effects and Specific Heparin Affinity. It has been shown for several cases that the effect of salt on protein−heparin interactions in homogeneous solution can be interpreted by polyelectrolyte theory (*37*). This theory assumes that proteins displace ions that are electrostatically bound to heparin and, more specifically in this case, that proteins compete with sodium ions for the binding sites on the heparin chain. According to this theory, a graph of log K_d versus log [Na] should be linear, and the slope should indicate the number of electrostatic interactions between the protein and heparin [log K_d = log K_d^0 + $z\Psi$ log M^+, where z = the number of displaced ions, Ψ = the axial charge density (Ψ = 0.8 for heparin), and K_d^0 = the contribution of nonionic interaction at M^+ = 0] (*37*). The polyelectrolyte theory

appears to be applicable to rhEC-SOD at salt concentrations at and above physiological salt concentration. Assuming that the number of displaced ions (z) in the equation above must take an integer value (shown as different slopes in Figure 4), it appears that a z-value of 2 would give the best fit to the experimental points. This appears to fit the models presented by Margalit and Mulloy (*28*, *29*), who predict that two basic amino acid residues at specific structural positions are required for a specific interaction between a protein and heparin/heparin sulfate.

However, at low salt concentrations the K_d of the EC-SOD−heparin interaction at the sensorchip surface showed little sensitivity to salt. Consequently, for rhEC-SOD the polyelectrolyte theory does not adequately describe the protein−heparin interaction at low salt concentrations. The observation that salt can decrease the number of binding sites has also been shown for LPL−heparin interactions at the sensorchip surface (*17*) and for protein interactions with charged lipids (*38*). The authors of the lipid study explain the latter phenomenon by the nonlocalized binding sites model, which includes competition between binding forces, and lateral interactions between bound proteins at surfaces. Recently, Xu and Yeung (*39*) showed that charged surfaces can influence charged proteins at distances beyond that of the electrical double-layer thickness, leading to long-range electrostatic trapping of protein molecules. Considering our data together with observations in the literature, we propose that protein interactions with immobilized heparin are complex and include both specific binding and nonspecific, and possibly also nonlocalized, long-range effects.

The salt effects on heparin binding to FusCC and the synthetic peptide (Figure 4) are different from the results on rhEC-SOD and are difficult to interpret. For example, salt might affect the conformation of the peptide (the ratio between $C_{\text{high affinity}}$ and $C_{\text{low affinity}}$, Scheme 1).

Further studies of the hEC-SOD/heparin interaction will include kinetic and structural studies of variants which are modified in the C-terminal domain.

ACKNOWLEDGMENT

The skillful technical assistance of Katarina Wallgren is gratefully acknowledged. We also thank Dr. Bengt-Harald Jonsson for helpful discussions, Dr. Gunilla Olivecrona for valuable support, and Dr. Per Østergaard for kindly providing the purified heparin fragments.

REFERENCES

1. Conrad H. E., Heparin binding proteins. (1998) *Academic Press*, San Diego.
2. Faham S., Hileman R. E., Fromm J. R., Linhardt R. J., and Rees D. C. (1996) *Science 271*, 1116−1120.
3. Digabriele A. D., Lax I., Chen D. I., Svahn C. M., Jaye M., Schlessinger J., and Hedrickson W. (1998). *Nature* 393: 812−817.
4. Marklund S. L. (1982) *Proc. Natl. Acad. Sci. U.S.A. 79*, 7634−7638.
5. Karlsson K., Lindahl U., and Marklund S. L. (1988), *Biochem. J. 256*, 29−33.
6. Tibell L. A. E., Sethson I., Buevich A. V. (1997) *Biochim Biophys Acta 1340*, 21−32.
7. Hjalmarsson K, Marklund S. L., Engström Å., and Edlund T. (1987) *Proc. Natl. Acad. Sci. U.S.A. 84*, 6340−6344.
8. Sandström J., Carlsson L., Marklund S., and Edlund T. (1992) *J. Biol. Chem. 267*, 18205−18209.
9. Sandström J., Nilsson P., Karlsson K., and Marklund S. M. (1994) *J. Biol. Chem. 269*, 19163−19166.
10. Ohta H., Adachi T., and Hirano K. (1993) *Free Radical Biol., & Medicine 15*, 151−158.
11. Karlsson K., Edlund A., Sandström J., and Marklund S. (1993) *Biochem. J. 290*, 623−626.
12. Inoue M., Nobukazu W., Matsuno K., Sasaki J., Tanaka Y., Hatanaka H., and Amachi T. (1991) *J. Biol. Chem. 266*, 16409−16414.
13. Gao B., Flores S. C., and McCord J. M. (1995) *Biol. Trace. Elem. Res. Jan-Mar 47*, 95−100.
14. Stenlund P., and Tibell L. A. E. (1999) *Protein Eng. 12*, 319−325.
15. Larnkjaer, A., Nukjaer, A., Olivecrona, G., Thorgersen, H., and Østergaard, P. B. (1995) *Biochem. J. 307*, 205−14.
16. Edlund, A., Edlund, T., Hjalmarsson, K., Marklund, S. L., Sandström, J., Strömqvist, M., and Tibell, L. (1992) *Biochem. J. 288*, 451−456.
17. Lookene, A., Chevreuil, O., Ostergaard, P., Olivecrona G. (1996) *Biochemistry 35*, 12155−12163.
18. Hall, D. R., Cann, J. R., and Winzor, D. J. (1996) *Anal. Chem. 235*, 175−184.
19. Garnier, J., Gibrat, J. F., and Robson, B. (1996) *Methods in Enzymology, R. F. Doolittle E. 266*, 540−553.
20. Muñoz, V., and Serrano, L. (1994). *J. Mol. Biol 245*, 275−296.
21. Muñoz, V., and Serrano, L. (1994). *J. Mol. Biol 245*, 297−308.
22. Muñoz, V., and Serrano, L. (1997). *Biopolymers 41*, 495−509.
23. Lacroix, E., Viguera, A.R., and Serrano, L. (1998). *J. Mol. Biol. 284*, 173−191.
24. Chakrabartty A., Schellman J. A., and Baldwin R. L. (1991) *Nature 351*, 586−8.
25. Luo P., and Baldwin R. L. (1997) *Biochemistry 36*, 8413−8421.
26. Holtzer, M. E., and Holtzer, A. (1992) *Biopolymers 32*, 1675−7.
27. Cardin, A. D., and Weintraub, H. J. R. (1989) *Arteriosclerosis 9*, 21−32.
28. Margalit, H., Fischer, N., and Ben-Sasson, S. A. (1993) *J Biol. Chem. 268*, 19228−31.
29. Mulloy, B., Crane, D. T., Drake, A. F., and Davis, D−B. (1996) *Braz J Med Biol Res 29*, 721−729.
30. McGhee, J. D., and von Hippel, P. H. (1974) *J.mol. Biol, 86*, 469.
31. Mach, H., Volkin, D. B., Burke, C. J., and Middaugh, C. R. (1993) *Biochemistry 32*, 5480−5489.
32. Lyon, M., Deakin, J. A., Rahmoune, H., Fernig, D. G., Nakamura, T., and Gallagher, J. T. (1998) *J. Biol. Chem. 2*, 271−278.
33. Muños, V., and Serrano, L. (1994) *Nature Struct. Biol. 1*, 399−409.
34. Ferran, D. S., Sobel, M., and Harris, R. B. (1992) *Biochemistry 31* 5010−16.
35. Ingham, K. C., Brew, S. A., and Atha, D. H. (1990) *Biochem. J. 272*, 605−611.
36. Lennick, M., Brew, S. A., and Ingham, K. C., (1986) *Biochemistry 25*, 3890−3898.
37. Olsson, S. T., Halvorson, H. R., and Björk, I. (1991) *J. Biol. Chem 266*, 6342−6352.
38. Heimburg, T.; March, D. (1995) *Biophys. J. 68*, 536−546.
39. Xu, X−H. N., and Yeung, E. S. (1998) *Science 281*, 1650−1653.

BI991512X